

**Catalytic hydrodeoxygenation of benzoic acid as a bio-oil model
compound: Reaction and kinetics using nickel-supported catalysts**

Mustapha Yusuf^{1,2}, Gary Leeke¹, and Joseph Wood^{1*}

¹School of Chemical Engineering, University of Birmingham, Edgbaston, Birmingham B15
2TT, United Kingdom

²Department of Chemical Engineering, Ahmadu Bello University, Zaria, 810261, Nigeria

Supplementary Information

Table S1 Textural properties of ZSM-5 and SiO₂ supports and their prepared Ni-based catalysts.

Sample	S_{BET}	S_{ext.}	V_{total}	V_{meso}	Pore width avg.	Acidity
	(m² g⁻¹)^a	(m² g⁻¹)^b	(m³ g⁻¹)^c	(m³ g⁻¹)^d	(nm)^e	(a.u.)^f
m-ZSM-5	434	158	0.284	0.137	3.98	4018
h-ZSM-5	459	221	0.342	0.216	4.63	4465
h-Ni/ZSM-5	316	150	0.257	0.169	4.97	4967
m-Ni/ZSM-5	378	142	0.235	0.109	3.68	5289
SiO₂	248	237	0.642	0.638	10.43	562
Ni/SiO₂	232	222	0.594	0.591	10.31	898

^aFrom N₂ adsorption measurement. ^bFrom N₂ adsorption measurement (t-plot). ^cFrom N₂ adsorption measurement at P/P₀ = 0.8942. ^dDifference between c and d (V_{total} - V_{micro}). ^eFrom BJH method. ^fTPD-Total peak area.

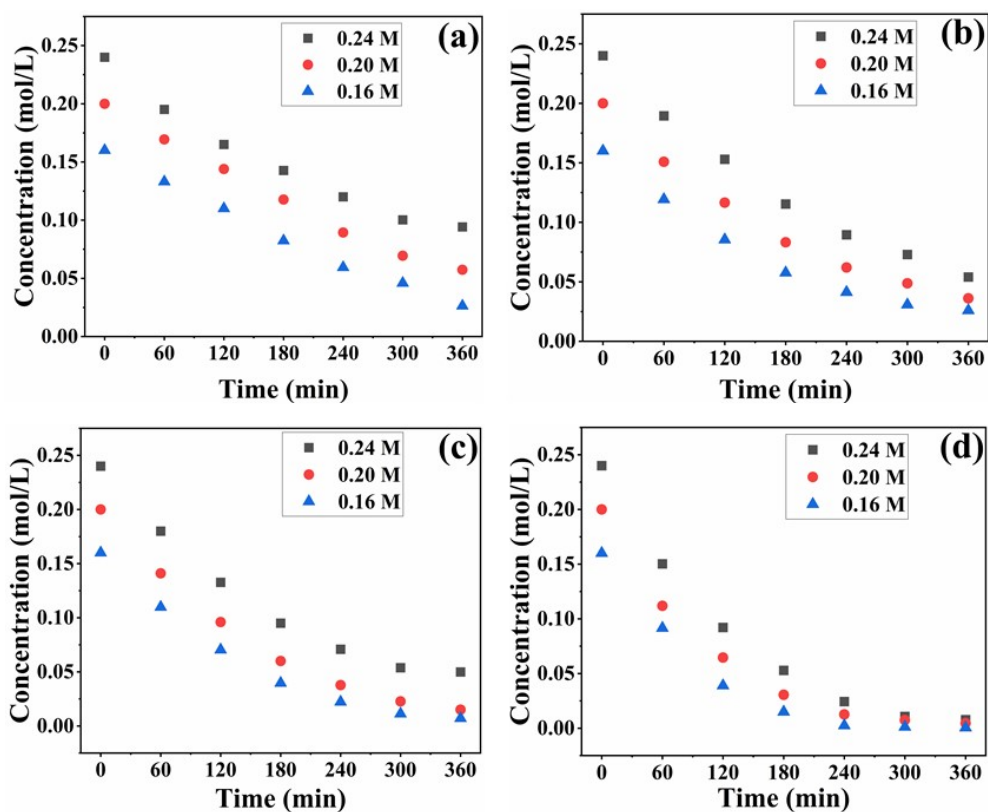


Figure S1. Concentration versus time profile for the benzoic acid hydrodeoxygenation, initial concentration of benzoic acid, 0.16 – 0.24 M; catalyst loading, 100 mg h-Ni/ZSM-5; stirring rate, 800 rpm; reaction pressure, 60 bar H₂; solvent, tetralin; reaction temperature, (a) 310 °C, (b) 320 °C, (c) 330 °C, and (d) 340 °C.

Table S2 Concentration of dissolved hydrogen in tetralin at different hydrogen pressure.

Temp. (°C)	Pressure (bar)	C_{H_2} (mM)
330	20	39.84
330	40	59.76
330	60	67.94

Table S3 Product distribution as a function of temperature during the HDO of benzoic acid over 5 wt.% nickel-based h-Ni/ZSM-5: Catalyst loading; 100 mg, solvent; tetralin, benzoic acid initial concentration; 0.16 M, reaction time; 6 hours.

Temp. (°C)	320	330	340
Conversion (%)	83.8	95.2	99.6
	Product distribution (%)		
Benzene	19.1	23.7	27.6
Toluene	45.2	38.1	36.9
Cyclohexane	1.9	3.7	1.4
Benzaldehyde	20.2	15.5	17.3
Benzyl alcohol	13.6	19.1	16.8

The Anderson¹ equation (eqn. S1) was used to evaluate the degree of metal dispersion.

$$D = \frac{6V_m}{d_{av}A_m} \quad \text{S1}$$

Where V_m is the atomic volume of nickel (0.0109 nm³), A_m is the surface area of single atom (0.0649 nm² for nickel), and d_{av} is the average diameter of the metal particle determined from the TEM analysis of the catalyst.

Calculation of Hydrogen Concentration Using Fogg and Gerrard Correlations

The equations below (eq. S2 and S3) present Fogg and Gerrard correlations used to determine the value of hydrogen concentration in mg L⁻¹;^{2,3}

$$C_{H_2} = y_{H_2} \times \frac{P_{total}}{P_{total} = 1bar} \times \frac{x_{H_2}}{1 - x_{H_2}} \times \rho_s \frac{M_{H_2}}{M_s} \times 1000 \quad S2$$

$$x_{H_2} = \exp \left(-125.939 + \frac{5528.45}{T} + 16.8893 \times \ln(T) \right) \quad S3$$

where C_{H_2} is the concentration of hydrogen, y_{H_2} is the mole fraction of hydrogen in the gas phase, x_{H_2} is the mole fraction of hydrogen in the liquid phase, ρ_s is the density of solvent in $g L^{-1}$, M_{H_2} is the molar mass of hydrogen in $g mol^{-1}$, M_s is the molar mass of solvent in $g mol^{-1}$, and T is the reaction temperature in Kelvin.

Given the following constants;

$$P_{Total} = 60 \text{ bar}$$

$$\rho_s = 973 \text{ g L}^{-1}$$

$$M_{H_2} = 2.016 \text{ g mol}^{-1}$$

$$M_s = 132.2 \text{ g mol}^{-1}$$

While values for x_{H_2} were determined from equation S3 at different temperatures shown in Table S3, values for y_{H_2} at the corresponding temperatures were obtained from solubility data for the tetralin-hydrogen system available in solubility data series volume 5/6.⁴

Table S4 Hydrogen concentration in tetralin solvent at different reaction temperature.

Temp. °C	Temp. K	y_{H_2}	x_{H_2}	$C_{H_2}(\text{mol L}^{-1})$
310	583	0.8195	0.000136114	0.049265728
320	593	0.7949	0.000154597	0.054276824

330	603	0.7702	0.000175678	0.059762649
340	613	0.7456	0.000199713	0.06577049

Calculation of Diffusion Coefficient (D_{ei}) and the Observable Modulus ($\eta\phi^2$)

Diffusivities in liquid can be calculated from different correlations that are available. Díaz et al.⁵ is one of the most widely used correlation to calculate the diffusivity of gases in liquid over wide temperature range. For accuracy, this correlation considered diffusivity at both 25 °C and the actual reaction temperature as states by equation S4 and S5 This is applied here to determine the coefficient of hydrogen and benzoic acid in tetralin;

$$(D_{ei})_{T=25\text{ }^\circ\text{C}} = 6.02 \times 10^{-5} \frac{V_A^{0.36}}{\mu_A^{0.61} V_i^{0.64}} \quad \text{S4}$$

$$(D_{ei})_T = 4.996 \times 10^3 \times [(D_{ei})_{T=25}] \times e^{-\frac{2539}{T}} \quad \text{S5}$$

where $(D_{ei})_T$ is the diffusion coefficient of reactant i (hydrogen and benzoic acid) in solvent A (tetralin) (at a given temperature T in $\text{cm}^2 \text{ s}^{-1}$, $(D_{ei})_{T=25\text{ }^\circ\text{C}}$ is the diffusion coefficient at 25 °C in $\text{cm}^2 \text{ s}^{-1}$, T is absolute temperature in Kelvin, μ_A is the viscosity of tetralin in cP, V_i is the molar volume of reactant at the normal boiling point temperature in $\text{cm}^3 \text{ gmol}^{-1}$, and V_A is the molar volume of tetralin at normal boiling temperature in $\text{cm}^3 \text{ gmol}^{-1}$.

Hence

$$V_{H_2} = 23.8 \text{ cm}^3 \text{ gmol}^{-1}$$

$$V_{BA} = 92.5 \text{ cm}^3 \text{ gmol}^{-1}$$

$$V_A = 135.7 \text{ cm}^3 \text{ gmol}^{-1}$$

$$\mu_A = 2.02 \text{ cP}$$

Therefore,

$$(D_{eH2})_{T=25\text{ }^\circ\text{C}} = 2.67 \times 10^{-9} \text{ m}^2 \text{ s}^{-1}$$

$$(D_{eBA})_{T=25\text{ }^\circ\text{C}} = 1.27 \times 10^{-9} \text{ m}^2 \text{ s}^{-1}$$

Detailed Discussion About Diffusion Control

In heterogeneous catalysis involving solid-liquid-gas phases present, it is imperative to maintain the solid catalyst in suspension for effective contact and subsequent reactions. This is achieved in agitated reactors by rotating impellers. Thus, a critical impeller speed (N_{js}) defined by equation 4 was determined. The results revealed that only 19, 20, or 21 rpm are needed to retain the h-Ni/ZSM-5 catalyst with particle sizes of 75 – 90 μm , 90 – 120 μm , or 120 – 140 μm in suspension during the benzoic acid HDO experiments. However, these minimum stirring speeds observed in this work are far lower than what was reported by Lawal et al.⁶ for the hydrogenation of acetic acid over a 4% Pt/TiO₂ catalyst. The lower values of N_{js} obtained in this study may be associated with the nature of the 5% h-Ni/ZSM-5 catalyst and the properties of solvent (e.g., density and viscosity) used as the reaction medium. Although this is true, it does not completely eliminate the possibility that external mass transfer limitations may exist within the reaction mixture. Arora et al.⁷ Arora noted that at a stirring speed of 500 rpm, there was limited hydrogen transfer across the gas-liquid boundary and potentially to the catalyst surface during the HDO of stearic acid. Despite this speed being above the minimum required to maintain the catalyst in suspension, the product yield was similar to that at low hydrogen pressure, indicating a restricted hydrogen supply to the catalyst surface and a low rate of product turnover. Therefore, the effect of varying stirring speeds on benzoic acid reaction rates was examined.

A range of stirring speeds from 400 rpm to 1000 rpm was investigated experimentally to examine how stirring speed affects benzoic acid conversion and initial rate during the HDO reaction. By fitting a polynomial to the concentration-time data, the initial reaction rate was determined using the differentiation method described in the literature.^{6,8} The experimental results are presented in Fig. 5a. Both the initial rate of reaction and benzoic acid conversion increase as the impeller stirring rate increases from 400 rpm to 800 rpm. Conversion was 54.3%, 77.1% 96.4% and 95.2% at 400, 600, 800, and 1000 rpm respectively. Similarly, the initial rate of benzoic acid HDO reaction plateaued at 800 rpm ($1.44 \times 10^{-3} \text{ mol L}^{-1} \text{ min}^{-1}$). Notably, the initial reaction rate and conversion were unaffected by the further increase in impeller speed from 800 rpm to 1200 rpm. As a result, impeller speeds of 800 rpm and above seem to eliminate external transport limitations during HDO of benzoic acid, which is a three-phase reaction of gas-liquid-solid phases. Accordingly, the subsequent results reported in this paper are based on experiments performed at an impeller speed of 800 rpm.

The results of the effect of particle size distribution on benzoic acid conversion and initial reaction rates are shown in Fig. 5b. In a catalytic reaction process, one of the major factors that determines the extent of the transformation a reactant undergoes is its ability to reach the catalytically active sites. Among the problems caused by internal transport limitations is pore diffusion, which can severely slow down the reaction rate.^{4,9} Herein, the reaction rate is greatly influenced by the pace at which hydrogen and benzoic acid diffuse through the porous network of the 5% h-Ni/ZSM-5 catalyst. Thus, it is critical to eliminate intraparticle diffusion resistance in order to ensure the HDO of benzoic acid is happening in a kinetically controlled regime. Hence, the effect of catalyst particle size on the rate of benzoic acid disappearance was

examined. It is believed that as the particle size decreases, the diffuse path length to the active sites within the catalyst decreases, thereby reducing intraparticle diffusion.

Prior to the reaction, the catalyst powder was sieved into the following particle size distributions: $75 \mu\text{m} < d_p < 90 \mu\text{m}$, $90 < d_p < 120 \mu\text{m}$, and $120 \mu\text{m} < d_p < 140 \mu\text{m}$, respectively. The catalyst was then activated at $500 \text{ }^\circ\text{C}$. Benzoic acid conversion was 79.5%, 79.4% and 68.7% while the initial reaction rate was 1.075×10^{-3} , 1.074×10^{-3} , and $1.051 \times 10^{-3} \text{ mol L}^{-1}\text{min}^{-1}$ respectively, for $75 \mu\text{m} < d_p < 90 \mu\text{m}$, $90 < d_p < 120 \mu\text{m}$, and $120 \mu\text{m} < d_p < 140 \mu\text{m}$ particle sizes. It is obvious that both the conversion and initial reaction rate are similar for 5% h-Ni/ZSM-5 catalyst particle size $75 \mu\text{m} < d_p < 90 \mu\text{m}$ and $90 < d_p < 120 \mu\text{m}$. This result shows that catalyst particles with a diameter of less than or equal to $120 \mu\text{m}$ eliminate intraparticle diffusion limitations.

To further confirm the absence of intraparticle diffusion, a criterion suggested by Weisz and Prater¹⁰ was deployed. This states that if the value of the observable modulus ($\eta\phi^2$), as defined in equation 5, is less than 0.3 for a reaction order of less than or equal to 2, the effect of internal diffusion is eliminated. Then the experimental data are appropriate for kinetic model development. Fogg and Gerrard correlations were employed to determine the value of hydrogen concentration, C_{H_2} , in mg L^{-1} .^{3,11,12} The mole fraction of hydrogen in the liquid phase was obtained from solubility data for the tetralin-hydrogen system available in solubility data series volume 5/6 (International Union of Pure and Applied Chemistry). Table 3 displays the Weisz-Prater values for both hydrogen and benzoic acid reactants at the different reaction temperatures investigated. The results show that the value of Weisz-Prater is significantly lower than 0.3, which agrees with the results presented in Fig. 5, implying that at 800 rpm and

catalyst particles with a diameter of less than or equal to 120 μm both external and internal mass transport limitations are eliminated.

References

- 1 J. R. Anderson, *Acad. Press. Lodon*, 1975, **55**, 86.
- 2 A. Pintar, G. Berčič and J. Levec, *AIChE J.*, 1998, **44**, 2280–2292
- 3 S. Srivastava, G. C. Jadeja and J. K. Parikh, *Int. J. Chem. React. Eng.*, 2018, **16**, 20170197.
- 4 C. G. Hill, *Solubility Data Series (Volume 5/6)*, Pergamon Press, U.K., 1981.
- 5 A. V. Mario Díaz and J. Coca, *Chem. Eng. Commun.*, 1987, **52**, 271–281.
- 6 A. M. Lawal, A. Hart, H. Daly, C. Hardacre and J. Wood, *Energy and Fuels*, 2019, **33**, 5551–5560.
- 7 P. Arora, E. L. Grennfelt, L. Olsson and D. Creaser, *Chem. Eng. J.*, 2019, **364**, 376–389.
- 8 H. S. Fogler, *Elements of Chemical Reaction Engineering*, 2019.
- 9 H. S. Fogler, *Elements of Chenzicn I Reaction Engineering*, 2006.
- 10 P. B. Weisz and C. D. Prater, eds. W. G. Frankenburg, V. I. Komarewsky and E. K. B. T.-A. in C. Rideal, Academic Press, 1954, vol. 6, pp. 143–196.
- 11 A. Pintar, G. Berčič and J. Levec, *AIChE J.*, 1998, **44**, 2280–2292.
- 12 P. Chang and C. R. Wilke, *AIChE J.*, 1955, 264–270.